J Mol Model (2007) 13:367–379
DOI 10.1007/s00894-006-0151-x

ORIGINAL PAPER

Pt-bridges in various single-strand and double-helix DNA sequences. DFT and MP2 study of the cisplatin coordination with guanine, adenine, and cytosine

Matěj Pavelka · Jaroslav V. Burda

Received: 28 December 2005 / Accepted: 23 June 2006 / Published online: 20 September 2006

Abstract In this study, various platinum cross-links in DNA bases were explored. Some of these structures occur in many *cis*/*trans*-platinated double-helixes or single-stranded adducts. However, in the models studied, no steric hindrance from sugar-phosphate backbone or other surroundings is considered. Such restrictions can change the bonding picture partially but hopefully the basic energy characteristics will not be changed substantially. The optimization of the structures explored was performed at the DFT level with the B3LYP functional and the 6-31G(d) basis set. Perturbation theory at the MP2/6-31++G(2df,2pd) level was used for the single-point energy and 6-31+G(d) basis set for the electron-property analyses. It was found that the most stable structures are the diguanine complexes followed by guanine-cytosine Pt-cross-links, ca 5 kcal mol^{-1} less stable. The adenine-containing complexes are about 15 kcal mol^{-1} below the stability of diguanine structures. This stability order was also confirmed by the BE of Pt–N bonds. For a detailed view on dative and electrostatic contributions to Pt–N bonds, Natural Population Analysis, determination of electrostatic potentials, and canonical Molecular Orbitals description of the examined systems were used.

Keywords *Cis*platin crosslinks · DFT calculations · MP2 calculations · DNA bases · Stabilization energy

Proceedings of "Modeling Interactions in Biomolecules II", Prague, September 5th–9th, 2005.

M. Pavelka · J. V. Burda (✉)
Faculty of Mathematics and Physics,
Department of Chemical Physics and Optics, Charles University,
Ke Karlovu 3,
121 16 Prague 2, Czech Republic
e-mail: Burda@karlov.mff.cuni.cz

Introduction

Platinum complexes represent one of the very promising classes for antitumor treatment since Rosenberg's [1] discovery. Many platinum compounds involving both Pt (II) and Pt(IV) have been examined since. Oncological in vivo research is supported by many in vitro experiments on oligo—and polynucleotides, see e.g. [2–10] Some more detailed insight into the physico-chemical description can also be achieved by computational techniques, which reveal structural and bonding relations in platinum complexes. Because of its high toxicity and resistance of tumor cells to *cis*platin when administered repeatedly, the applicability and properties of many derivatives of *cis*platin have been explored. In this way, second- and later third-generation drugs (like carboplatin, oxaliplatin, Pt(IV) complex JM216 or trinuclear BBR 3464) were discovered. At present, *cis*platin and carboplatin belong to the most often used drugs [11]. The final DNA adduct of both (and some other platinum drugs, too) includes the same *cis*-[Pt(NH_3)$_2$-1,2−d {GpG}]$^{2+}$ fragment. These adducts cause a roll of 25–50° between the guanine bases involved in the cross-link and a global bend of the helix axis towards the major groove of about 20–40° [12–16]. The molecular structure of this complex was solved by the Dickerson group at high resolution (2.6 Å) [17]. A similar structure, which also contains the *cis*platin G–Pt–G bridge [12], was measured with the same resolution. The distortion of DNA under the influence of *cis*platin was found by Lilley [18]. The structure of the interstrand *cis*platin bridge was published in Ref. [19] and the cross-linked adduct of oxaliplatin with 1,2−d(GpG) intrastrand bases of the DNA oligomer was studied by the Lippard's group [20]. Afterwards, some other platinum complexes were crystallized and described [21, 22]. The ternary complex of a DNA oligomer with

*cis*platin and HMG-protein was prepared and its crystal structure was solved and reported [23, 24].

Six-coordinated platinum(IV) complexes have also been explored extensively recently [25–29]. These complexes are relatively stable and can be passed through the digestive tract. After absorption into the bloodstream, they are metabolized and reduced to four-coordinated *cis*platin analogues [30]. Recent reviews of Wong [31] and Reedijk [32] summarize the current state of platinum-drug treatment. Another study of Reedijk deals with competition between S-donor ligands and DNA [33]. The interstrand cross-linked binding of DNA bases with *trans*platin complexes was studied in detail by Brabec [34]. Quaternary platinum complexes in solution were explored by Sigel and Lippert [35]. Various conformers of the *cis*platin adduct with d(GpG) were examined by the Marzilli group [36], where the phosphodiester backbone conformation was also discussed. In this study, they combined several experimental tools (NMR (^{1}H and ^{31}P), CD spectroscopy) with simulation based on molecular mechanics (MM) and molecular dynamics (MD).

*Cis*platin can also form interstrand cross-links as a minor adduct [37, 38] where complementary cytosines are extruded from the double helix. This link bends the helix axis towards the minor groove by 30–50° and unwinds the duplex by more than 80°. The formation of the interstrand platinum bridges can be as fast as the formation of intrastrand cross-links for short DNA oligomers [39–41]. The interstrand *cis*platin cross-links are unstable under physiological conditions [42], leading to monofunctional adducts. The difference between the interstrand and intrastrand Pt-bridges can be distinguished through the mutual orientation of the guanine bases. While intrastrand Pt-complexes contain a head-to-head orientation, in interstrand complexes *cis*platin usually forms a head-to-tail orientation of the bases.

In the *trans*platin case, the formation of the monofunctional adduct takes about 2–3 h, similarly to the *cis*platin complex [43]. The *trans*platin complexes evolve slowly (T_{12}=40 h) and interstrand cross-links between guanine and complementary cytosine residues are formed [44]. 2D-NMR confirms the *trans*-[Pt$(NH_3)_2$(N7-guanine)(N3-cytosine)]$^{2+}$ structure with guanine in the syn-conformation [45]. However, the formation of 1,3- and longer intrastrand platinum cross-links was described in another study [40]. Similar Pt-bridges were found in single-stranded DNA chains where sequences GXG also occur. However, such 1,3−d(GpXpG) bridges are not stable. When a cytosine base is in the adjacent position to the 5′-end guanine, a new cross-link 1,4-d(CpGpXpG) can be formed and equilibrium between these two structures is attained [46, 47]. The same instability was also observed in DNA duplexes where 1,3-intrastrand cross-link triggers isomerization reactions with rearrangement into interstrand cross-links [48, 49]. Interestingly, the cross-link is formed between the (less strongly bonded) 5′-end guanine base and complementary cytosine. An explanation for the preference of the 5′-end base consists of the steric conditions: this reaction represents a direct nucleophilic attack on the Pt–G(3′) bond by the cytosine residue opposite to G(5′) of the second DNA strand [50]. Considering the larger basicity of the N1 site over N7 site in the purine bases, the N7→N1 migration of Pt may be anticipated. In fact, this type of isomerization was observed in the Pt-complexes with inosine [51] or adenosine [52].

In the field of Pt-nucleobase interactions, there are also many computational studies. The complex of *cis*platin with 1,2-d(GpG) bases was examined by Carloni [53] who also considered some hydration aspects of *cis*platin using Car–Parrinello MD simulations. The effect of N7 platination on the strength of the N9–C1′ glycosyl bond of purine bases was revealed in the study of Baik [54]. In another work, the reaction mechanism of formation of the Pt$(NH_3)_2$ diguanine complexes was explored [55]. A similar study was performed by Eriksson [56] where both reaction steps that create monofunctional and bifunctional complexes were considered. The first step, the formation of a monofunctional adduct, was also explored by Chval [57]. The thermodynamics of Pt-bridges, bonding energy parameters, and the influence of a sugar-phosphate backbone were also studied in some of our other papers [58–60].

DFT techniques with the VTZP basis set were used recently by Deubel [61] to compare affinities of *cis*platin to S-sites and N-sites of amino acids and DNA bases. His results are in very good agreement with our previous calculations on the thermodynamics of platinum-complex hydration [62–65] as well as the interaction with sulphur-containing amino acids [66].

From all the examples of experimental works mentioned above, our motivation can be seen for a more extensive exploration of the close platinum vicinity. The bonding relations within the chosen Pt-bridges with two DNA bases need to be elucidated. The different base's orientations (HH or HT) correspond to different cross-link conditions in inter- and intrastrand Pt-bridges. Despite the fact that the geometric conditions play an important role in the cross-link formation, it can be expected that energetic and especially kinetic factors control the reaction course. This study clarifies the binding differences between individual Pt–N dative bonds in platinum coordination to various bases, which will be useful in future studies where some other factors (kinetic and steric effects from more extended models) of platinum cross-links will be examined.

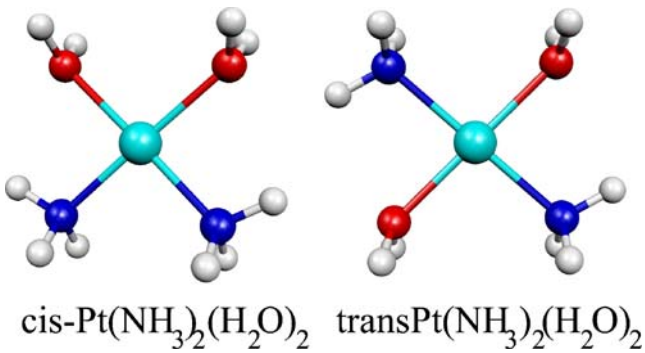

Scheme 1 Hydrated forms of *cis*/*trans*platin

Computational details

This study investigates various *cis*- and *trans*platin complexes with two DNA bases in both head-to-head (HH) and head-to-tail (HT) arrangements (the 2+ charged hydrated structures of *cis*-/*trans*-diaquadiammineplatinum complexes are shown in Scheme 1). All platinum complexes were in the singlet ground state with the total charge of +2, deprotonation of DNA bases under formation of platinum adducts was not confirmed by any experimental tool. The following bridged base pairs were explored: *cis*-/*trans*-$Pt(NH_3)_2$(N7-guanine)(N7-adenine), $Pt(NH_3)_2$(N7-guanine)(N3-cytosine), $Pt(NH_3)_2$(N1-guanine)(N3-cytosine), and $Pt(NH_3)_2$(N7-guanine)$_2$. In the case of N1(G) coordination, a proton from N1 nitrogen was transferred to the N7 atom, preserving the same total charge of the complexes. All the structures were optimized at the DFT level with the B3LYP functional and the 6-31G(d) basis set. Stuttgart–Dresden energy averaged relativistic pseudopotentials were used for the description of the Pt atom [67]. The original basis set of pseudoorbitals was augmented by a set of diffuse functions with exponents α_s=0.0075, α_p=0.013, and α_d=0.025, and the exponent α_f=0.98 was used for additional polarization functions.

Second order perturbation theory (MP2) was used for the single-point energy evaluations of the systems examined. In this case, the larger basis set 6-31++G(2df,2pd) was used. For further discussion, stabilization energies (ΔE^{Stab}), stabilization energies corrected on the steric repulsion of ligands and the presence of H–bonds (ΔE^{Stex}), and binding energies (BE) were computed. The ΔE^{Stab} and ΔE^{Stex} energies were calculated with the inclusion of the Basis Set Superposition Error corrections (BSSE) together with the inclusion of deformation-energy corrections according to the formula:

$$\Delta E^{x} = -\left(E_{complex} - \sum E_{fragment}\right) - \Delta E^{deform}. \quad (1)$$

x means the given type of stabilization energy. The sum of fragment energies contains energies of the Pt cation and the corresponding isolated ligands in the case of ΔE^{Stab}. In the case of ΔE^{Stex} energies, only two terms enter the summation of $E_{fragment}$—the energy of the isolated Pt cation and the energy of all the ligands in the optimized position taken as one (neutral) system. The contributions of deformation energies are very important: $\Delta E^{deform} = E^{ligand}_{complex-geom.} - E^{ligand}_{most-stable-comformer}$ since the difference between the optimized N7- and N1-conformers of guanine is also covered in this term. In the case of ΔE^{BE} evaluation, the same Eq. (1) was employed without the deformation term. In the calculations of ΔE^{BE}, the $E_{fragment}$ energies were determined in the space partitioning according to the examined Pt–L_4 bond: $[Pt–L_1L_2L_3]^{2+}$ and $[L_4]$. In all cases the $E_{fragment}$ energies are evaluated in the complex-optimized geometry with the complete set of ghost AO functions on the complementary part(s) of the complex.

Starting from the diammine-diaqua-platinum complex (*cis*-$[Pt(NH_3)_2(H_2O)_2]^{2+}$), two steps were considered, where both aqua ligands were replaced subsequently by a chosen base. Gibbs reaction energies were determined for this process within a microcanonical ensemble using ideal gas and harmonic oscillator models.

Partial charges were computed within the Natural Population Analyses (NPA) [68–70] using MP2/6-31+G (d) correlated wave functions. The standard atom numbering of the nucleobases is used throughout (cf. Scheme 2).

Donation and back-donation effects were investigated using the canonical MOs. Charge transfer (CT) from a base to the central metal was computed as a sum of NPA partial charges of the base in the given complex since all the bases are electroneutral when they are isolated. For a better

Scheme 2 DNA bases considered in the study with atom numbering of the heterocycles

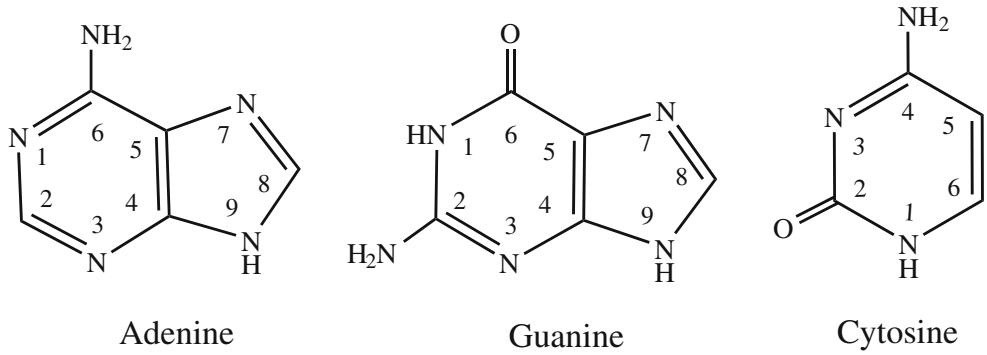

understanding of the systems studied, electrostatic potentials were mapped on the electron isodensity surfaces (ρ=0.001). All calculations were performed with the Gaussian 98 quantum chemical program package and the NBO v5.0 progam [71] was used for the NPA analyses. In this program, second order perturbative analysis of donor–acceptor interactions is available, labeled as E(2) energies. Using this tool, approximative values of Pt–N7(G), Pt–N7 (A) and Pt–N3(C) can be estimated.

Results

Structural parameters

The most important geometry parameters obtained from the complex optimizations are collected in Table 1. Besides distances of the Pt–N dative bonds, B–Pt–B valence angles and dihedral angles were chosen for discussion. From Table 1, we can see that Pt–N distances are shorter for the DNA base coordination than for the ammine ligands due to the possibility of back-donation in the case of nucleobases. The longest Pt–N bond (about 2.110 Å) was found for ammonia in the *trans*-$[Pt(NH_3)_2(N7\text{-guanine})_2)]^{2+}$ (HH) system. When the coordination distances for nucleobases are compared, the distinctly shortest Pt–N bonds can be found in the Pt–a_2GA systems. In the *cis*-$[Pt(NH_3)_2(N7\text{-guanine})(N7\text{-adenine})]^{2+}$ (HH) complex (Fig. 1-structure **1a**), the shortest Pt–N(adenine) bonds can be found (2.041 Å). The longest Pt–N distances (among the bases) occur in the cytosine complex of *cis*-$[Pt\text{–}a_2G(N7)C(N3)]^{2+}$.

Fig. 1 Diammine-platinum(II) cross-links with two DNA bases. ▶ Structures **a**, **b** represent *cis*platin head-to-head (HH), head-to-tail (HT) and structures **c**, **d** correspond to *trans*platin (HH), and (HT) conformers, respectively

In the complexes examined, the length of Pt–N dative bonds can be ordered: Pt–N7(A) (2.047 Å in average) <Pt–N7(G) (2.057) <Pt–N1(G) (2.069) <Pt–N3(C) (2.079) <Pt–N(a) (2.082 from the whole set of 32 bonds). The mutual repulsion between ammine ligand and protons of the NH_2 group of guanine, which is in the proximity of coordinated N1-site, is responsible for the fact that Pt–N1(G) bonds are longer than Pt–N7(G) in the Pt–a_2GC systems (especially in both *trans*platin complexes). The shortest Pt–N7(A) bond distance is supported by a better polarization of adenine (the largest change in the partial charge of N1 atom of adenine under platination among all partial charges from Table 2) and by larger E2 energies-cf. the discussion below.

From a detailed view on the Pt–N(ammine) bonds, one can recognize the changes caused by the influence of the H–bond of NH_3 ligands. The stronger the H–bond with an adjacent base, the shorter is the corresponding Pt–N(a) bond. The explanation lies in the reduction of N–H bond electron-density when its (ammine) hydrogen is involved in H–bonding. A higher effective electron density of N (ammine) can be used for donation to the Pt atom, resulting in a shorter Pt–N distance. The shortest Pt–N(a) bonds are about 2.075 Å (with H–bonds to the O6-guanine or O2-cytosine sites), while distances up to 2.11 Å can be seen for non-interacting ammine ligands. The strength of an H–bond also correlates indirectly with changes in the N–H stretching vibrations in comparison with isolated bases or ammonia

Table 1 Geometry parameters of investigated structures, Pt–$L_{1,2}$ and Pt–$B_{1,2}$ denote Pt–N bond lengths for ammonia ligands and nucleobases (in Å)

System	Pt–L_1	Pt–L_2		Pt–B_1		Pt–B_2		*D*1		*D*2	B_1–Pt–B_2
cis-Pt–a_2G(N7)A(N7) (HH)	2.089	2.095	G	2.041	A	2.044	G	−93.9	A	54.8	91.6
cis-Pt–a_2G(N7)A(N7) (HT)	2.087	2.076	G	2.058	A	2.053	G	−50.8	A	−50.1	91.1
trans-Pt–a_2G(N7)A(N7) (HT)	2.088	2.073	G	2.056	A	2.046	G	57.0	A	55.7	180.0
trans-Pt–a_2G(N7)A(N7) (HT)	2.088	2.072	G	2.057	A	2.046	G	−57.7	A	52.9	177.8
cis-Pt–a_2G(N7)C(N3) (HH)	2.082	2.077	G	2.058	C	2.083	G	−48.8	C	118.6	91.6
cis-Pt–a_2G(N7)C(N3) (HT)	2.075	2.085	G	2.062	C	2.084	G	−57.7	C	−111.5	92.7
trans-Pt–a_2G(N7)C(N3) (HH)	2.075	2.084	G	2.057	C	2.080	G	123.9	C	−56.4	178.0
trans-Pt–a_2G(N7)C(N3) (HT)	2.085	2.077	G	2.047	C	2.065	G	−66.3	C	−121.2	174.6
cis-Pt–a_2G(N7)G(N7) (HH)	2.074	2.074	G	2.065	G	2.065	G	60.9	G	−60.9	93.4
cis-Pt–a_2G(N7)G(N7) (HT)	2.073	2.073	G	2.061	G	2.061	G	−51.5	G	−51.4	90.1
trans-Pt–a_2G(N7)G(N7) (HH)	2.110	2.055	G	2.066	G	2.066	G	−51.1	G	51.1	175.0
trans-Pt–a_2G(N7)G(N7) (HT)	2.077	2.077	G	2.051	G	2.051	G	57.1	G	−57.1	180.0
cis-Pt–a_2G(N1)C(N3) (HH)	2.096	2.091	G	2.068	C	2.088	G	−88.5	C	123.2	93.1
cis-Pt–a_2G(N1)C(N3) (HT)	2.106	2.092	G	2.054	C	2.064	G	91.7	C	100.0	92.5
trans-Pt–a_2G(N1)C(N3) (HH)	2.081	2.080	G	2.083	C	2.086	G	−122.7	C	−132.4	175.3
trans-Pt–a_2G(N1)C(N3) (HT)	2.083	2.082	G	2.073	C	2.082	G	−126.1	C	121.1	178.8

*D*1 labels dihedral angles N(a)–Pt–N7–C5 (N(a)–Pt–N1–C6) of the base B_1 and *D*2 labels dihedral angles N(a)–Pt–N7–C5 (N(a)–Pt–N3–C4) of the base B_2, B_1–Pt–B_2 represents the angle between nucleobases.

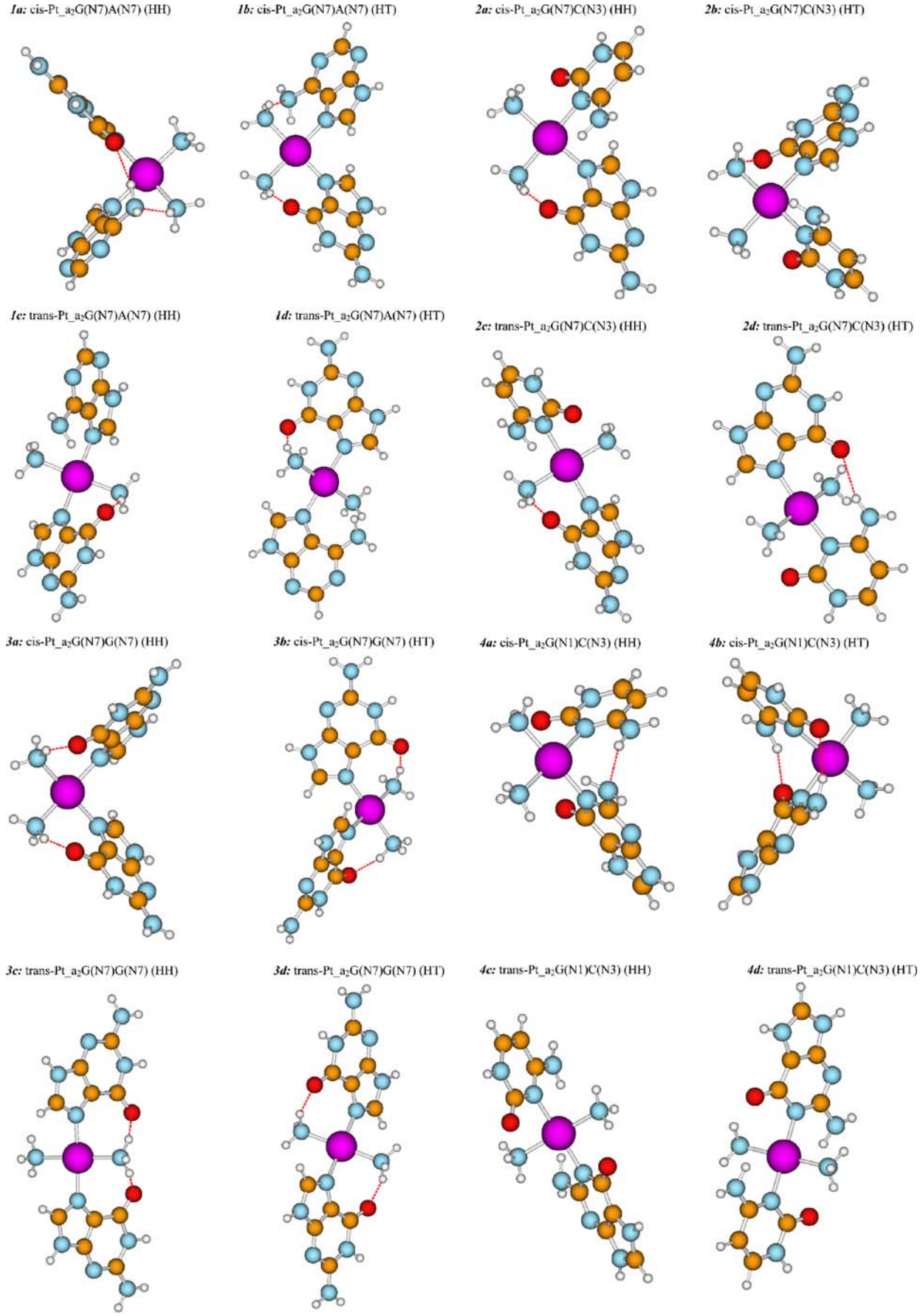
1a: cis-Pt_a2G(N7)A(N7) (HH)
1b: cis-Pt_a2G(N7)A(N7) (HT)
2a: cis-Pt_a2G(N7)C(N3) (HH)
2b: cis-Pt_a2G(N7)C(N3) (HT)
1c: trans-Pt_a2G(N7)A(N7) (HH)
1d: trans-Pt_a2G(N7)A(N7) (HT)
2c: trans-Pt_a2G(N7)C(N3) (HH)
2d: trans-Pt_a2G(N7)C(N3) (HT)
3a: cis-Pt_a2G(N7)G(N7) (HH)
3b: cis-Pt_a2G(N7)G(N7) (HT)
4a: cis-Pt_a2G(N1)C(N3) (HH)
4b: cis-Pt_a2G(N1)C(N3) (HT)
3c: trans-Pt_a2G(N7)G(N7) (HH)
3d: trans-Pt_a2G(N7)G(N7) (HT)
4c: trans-Pt_a2G(N1)C(N3) (HH)
4d: trans-Pt_a2G(N1)C(N3) (HT)

Table 2 Partial atomic charges on Pt, N(ammonia) and several important atoms of nucleobases: N7, N9, N2, N1, O6, H8, and H1 of guanine, N7, N9, N1, N6, and H8 of adenine, N3, N4, N1, O2, and H4 of cytosine (see Scheme 2), and charge transfer (CT) from base to Pt

System	Pt	N		N7/N3	N9/N4	N1	N7	X6/O2	H8	H1/H7	CT
cis-Pt–a_2G(N7)A(N7) (HH)	0.680	**−1.062**	G	**−0.485**	−0.530	−0.633	−0.813	−0.624	0.271	0.469	0.338
		−1.055	A	**−0.495**	−0.526	−0.459		−0.909	0.267		0.346
cis-Pt–a_2G(N7)A(N7) (HT)	0.673	**−1.056**	G	**−0.487**	−0.529	−0.628	−0.812	−0.616	0.269	0.472	0.358
		−1.056	A	**−0.512**	−0.525	−0.455		−0.898	0.264		0.337
trans-Pt–a_2G(N7)A(N7) (HT)	0.670	**−1.060**	G	**−0.487**	−0.528	0.635	−0.812	−0.625	0.271	0.471	0.348
		−1.051	A	**−0.505**	−0.523	−0.457		−0.897	0.272		0.346
trans-Pt–a_2G(N7)A(N7) (HT)	0.671	**−1.061**	G	**−0.485**	−0.528	−0.629	−0.812	−0.622	0.267	0.471	0.350
		−1.052	A	**−0.503**	−0.522	−0.457		−0.899	0.274		0.345
cis-Pt–a_2G(N7)C(N3) (HH)	0.673	**−1.054**	G	**−0.487**	−0.530	−0.629	−0.814	−0.622	0.272	0.471	0.346
		−1.049	C	**−0.627**	−0.785	−0.606		−0.610		0.448	0.331
cis-Pt–a_2G(N7)C(N3) (HT)	0.675	**−1.054**	G	**−0.482**	−0.530	−0.628	−0.815	−0.616	0.263	0.471	0.351
		−1.049	C	**−0.617**	−0.818	−0.601		−0.594		0.444	0.325
trans-Pt–a_2G(N7)C(N3) (HH)	0.667	**−1.057**	G	**−0.484**	−0.528	−0.630	−0.813	−0.613	0.268	0.471	0.355
		−1.056	C	**−0.618**	−0.802	−0.601		−0.604		0.444	0.342
trans-Pt–a_2G(N7)C(N3) (HT)	0.678	**−1.052**	G	**−0.485**	−0.530	−0.627	−0.813	−0.654	0.274	0.469	0.332
		−1.047	C	**−0.621**	−0.798	−0.604		−0.608		0.458	0.340
cis-Pt–a_2G(N7)G(N7) (HH)	0.688	**−1.052**	G	**−0.489**	−0.532	−0.630	−0.816	−0.613	0.271	0.470	0.338
		−1.052	G	**−0.489**	−0.532	−0.631	−0.816	−0.613	0.271	0.470	0.338
cis-Pt–a_2G(N7)G(N7) (HT)	0.689	**−1.050**	G	**−0.484**	−0.531	−0.632	−0.817	−0.611	0.258	0.469	0.334
		−1.050	G	**−0.484**	−0.531	−0.632	−0.817	−0.611	0.258	0.469	0.334
trans-Pt–a_2G(N7)G(N7) (HH)	0.687	**−1.074**	G	**−0.481**	−0.529	−0.634	−0.816	−0.596	0.261	0.469	0.342
		−1.033	G	**−0.481**	−0.529	−0.634	−0.816	−0.596	0.261	0.469	0.342
trans-Pt–a_2G(N7)G(N7) (HT)	0.688	**−1.057**	G	**−0.480**	−0.529	−0.631	−0.816	−0.619	0.271	0.469	0.345
		−1.057	G	**−0.480**	−0.529	−0.631	−0.816	−0.619	0.271	0.469	0.345
cis-Pt–a_2G(N1)C(N3) (HH)	0.666	**−1.061**	G	−0.471	−0.511	**−0.641**	−0.886	−0.569	0.292		0.374
		−1.053	C	**−0.612**	−0.786	−0.606		−0.614		0.447	0.328
cis-Pt–a_2G(N1)C(N3) (HT)	0.663	**−1.062**	G	−0.472	−0.515	**−0.624**	−0.836	−0.640	0.291		0.388
		−1.052	C	**−0.613**	−0.785	−0.607		−0.628		0.462	0.322
trans-Pt–a_2G(N1)C(N3) (HH)	0.648	**−1.047**	G	−0.470	−0.512	**−0.633**	−0.867	−0.619	0.293		0.381
		−1.055	C	**−0.620**	−0.802	−0.603		−0.602		0.440	0.322
trans-Pt–a_2G(N1)C(N3) (HT)	0.648	**−1.053**	G	−0.471	−0.512	**−0.628**	−0.870	−0.635	0.293		0.381
		−1.047	C	**−0.616**	−0.806	−0.602		−0.611		0.450	0.327
Isolated guanine(N7)			G	−0.448	−0.574	−0.661	−0.875	−0.573	0.236	0.448	
Isolated guanine(N1)			G	−0.477	−0.536	−0.615	−0.859	−0.641	0.2489	0.4781	
Isolated adenine			A	−0.493	−0.583	−0.534		−0.838	0.226		
Isolated cytosine			C	−0.591	−0.838	−0.634		−0.620		0.450	

In addition, partial charges of isolated bases are listed too. δ(N)=−1.136 e for ammonium molecule in vacuum. **Bold** font represents N atoms that coordinate to Pt (in e).

molecules. Some information can also be extracted from the changes in C=O and C–N6 vibration modes (cf. below).

An analysis of the bases' orientation and the H–bonding parameters represents a very interesting subject, which reflects several remarkable features. The distances of various H–bonds are shown in Table 3. In the *trans*platin complexes, the most frequent realization of H–bonding involves two H–bridges, both between an ammine-ligand and a DNA base: X...H–N(ammine) interaction (where X=guanine O6, adenine N6 or cytosine O2 site). In the *trans*-Pt–a_2G(N1)C(N3) complex, three for HH (Fig. 1 structure **4c**), and even four interactions of the X...H–N character for HT orientation (**4d**) can be noticed. Beside these two complexes, another interesting structure occurs in the *trans*-Pt–a_2G(N7)C(N3) (HT) complex (**2d**) where two X...H–N(ammine) interactions are accompanied by an additional (weaker) interbase H–bond (2.27 Å) O6...H–N4, which is the only *trans*platin complex with an interbase H–bond. This complex is also similar to the Hoogsteen base pairing, where a Pt cation mediates the N7(G)...N3(C) connection. The *trans*-Pt–a_2GG (HH) structure (**2c**) makes two H–bonds where the same ammine ligand is connected to both O6 atoms resulting in the shortest Pt–N(ammine) dative bond.

In the case of *cis*platin complexes, a larger variety of the base orientations can be observed. *Cis*platin complexes form interbase H–bonds more often. In the GA and G(N1)C complexes, relatively strong interbase H–bonds are present

Table 3 Hydrogen bonds X...H between ammine ligand and guanine O6, adenine N6 or cytosine O2 site

System		O6...H		O2/X6...H
cis-Pt–a_2G(N7)A(N7) (HH)	G	2.01(b)	A	2.09
cis-Pt–a_2G(N7)A(N7) (HT)	G	1.77	A	2.06
trans-Pt–a_2G(N7)A(N7) (HT)	G	1.87	A	2.14
trans-Pt–a_2G(N7)A(N7) (HT)	G	1.84	A	2.13
cis-Pt–a_2G(N7)C(N3) (HH)	G	1.82	C	2.05
cis-Pt–a_2G(N7)C(N3) (HT)	G	1.78	C	2.20
trans-Pt–a_2G(N7)C(N3) (HH)	G	1.80	C	2.00
trans-Pt–a_2G(N7)C(N3) (HT)	G	2.07/2.27(b)	C	2.04
cis-Pt–a_2G(N7)G(N7) (HH)	G	1.84	G	1.84
cis-Pt–a_2G(N7)G(N7) (HT)	G	1.80	G	1.80
trans-Pt–a_2G(N7)G(N7) (HH)	G	1.86	G	1.86
trans-Pt–a_2G(N7)G(N7) (HT)	G	1.85	G	1.85
cis-Pt–a_2G(N1)C(N3) (HH)	G	2.08(bN)[a]	C	1.95
cis-Pt–a_2G(N1)C(N3) (HT)	G	2.07(b)	C	1.89(b)
trans-Pt–a_2G(N1)C(N3) (HH)	G	1.88	C	2.15
trans-Pt–a_2G(N1)C(N3) (HT)	G	1.98	C	2.10

(b) labels the interbase interactions
[a] (bN) means interaction between N2(guanine)...H(N4-cytosine)

with O6...H(nucleobase) distance less than 2.10 Å. Structure **4b** partially resembles a bent Watson–Crick GC pair with two interbase H–bonds and the third base–base interaction is replaced by the Pt-cross-link. The *cis*-Pt–a_2G (N1)C(N3) is the only complex where other than the X6 atom of the DNA base is involved in the interbase H–bond. Here, an interaction between N2 atom of guanine and H (N4) of cytosine is established.

Energy analysis

Stabilization energies (ΔE^{Stab}, ΔE^{Stex}) and bonding energies (ΔE^{BE}) were evaluated for all complexes studied and are shown in Table 4.

Both *cis*- and *trans*platin complexes form fairly stable structures. Without the deformation corrections (ΔE^{deform}), the most stable compounds can be found in the group of Pt–a_2G(N1)C(N3) structures (the averaged ΔE^{Stab} is about 551 kcal mol^{-1}—not shown in Table 4). However, when the fact that the N1-conformer of guanine is about 18 kcal mol^{-1} less stable than the N7-conformer is

Table 4 ΔE^{Stab}, ΔE^{Stex} stabilization energies with and without inclusion of corrections on sterical repulsion, and bond energies ΔE^{BE}

System	ΔE^{Stab}	ΔE^{Stex}	ΔE^{BE}		ΔE^{BE}	
cis-Pt–a_2G(N7)A(N7) (HH)	535.8	547.9	G	112.5	A	95.0
cis-Pt–a_2G(N7)A(N7) (HT)	534.9	552.7	G	112.8	A	87.7
trans-Pt–a_2G(N7)A(N7) (HT)	536.7	552.6	G	113.9	A	90.9
trans-Pt–a_2G(N7)A(N7) (HT)	536.2	553.5	G	112.4	A	90.0
cis-Pt–a_2G(N7)C(N3) (HH)	545.2	560.3	G	112.1	C	100.2
cis-Pt–a_2G(N7)C(N3) (HT)	542.5	560.8	G	109.2	C	95.7
trans-Pt–a_2G(N7)C(N3) (HH)	545.4	562.5	G	110.3	C	100.9
trans-Pt–a_2G(N7)C(N3) (HT)	549.3	560.9	G	113.2	C	104.5
cis-Pt–a_2G(N7)G(N7) (HH)	551.1	573.9	G	103.2	G	103.2
cis-Pt–a_2G(N7)G(N7) (HT)	553.3	574.0	G	106.4	G	106.5
trans-Pt–a_2G(N7)G(N7) (HH)	547.8	571.4	G	104.3	G	104.3
trans-Pt–a_2G(N7)G(N7) (HT)	554.6	574.3	G	109.0	G	109.0
cis-Pt–a_2G(N1)C(N3) (HH)	552.8	568.7	G	120.0	C	99.6
cis-Pt–a_2G(N1)C(N3) (HT)	563.0	565.5	G	132.5	C	107.5
trans-Pt–a_2G(N1)C(N3) (HH)	558.0	575.3	G	124.1	C	93.8
trans-Pt–a_2G(N1)C(N3) (HT)	562.1	574.9	G	127.4	C	96.3

All values are in kcal mol^{-1}.

considered (which is included in the ΔE^{deform} term), the most stable complexes become the Pt–a_2GG systems. This holds for both the ΔE^{Stab} and ΔE^{Stex} values. An about 5 kcal mol^{-1} weaker stabilization was achieved in the case of Pt–a_2G(N7)C(N3) complexes. The structures with N1 coordination are on average about another 7 kcal mol^{-1} less stable than the corresponding G(N7) conformers. The least stable systems are the adenine-containing complexes (about 527 kcal mol^{-1}). This order is in good agreement with many previous studies on this subject.

Thanks to the formation of two strong interbase H–bonds: O6(G)...HN4(C) and O2(C)...HN2(G), the *cis*-Pt–a_2G(N1)C(N3) (HT) complex displays an exceptionally low steric repulsion; the difference between ΔE^{Stab} and ΔE^{Stex} energies, is only about 2.5 kcal mol^{-1}.

The strongest coordination to Pt is represented by the Pt–N1 bonds in Pt–a_2G(N1)C(N3) complexes, where the BE is about 126 kcal mol^{-1}. The highest BE energy is in the *cis*Pt–a_2G(N1)C(N3) (HT) complex. However, the Pt–N bonding is accompanied by two additional (relatively strong) interbase H–bonds. In the case of analogous Pt–a_2G(N7)C(N3) complexes, the ΔE^{BE} of Pt–N7(G) bonds are about 13 kcal mol^{-1} lower. The Pt–N3(C) exhibits very similar BE characteristics in both G(N1) and G(N7) conformers (about 100 kcal mol^{-1}). The explanation for the reduction of Pt–N7(G) BE can be seen in a lower electrostatic contribution. Considering the dipole moment of neutral conformers of guanine, a more advantageous interaction site for a positively charged Pt complex is N1 in the N1-conformer (with the N7 site protonated). The dipole moment is oriented in the N1→N9 direction and its value is about 9.5 D (B3LYP/6-31G+(d), cf. Fig. 2), while the regular N7 conformer has dipole μ=6.8 D with orientation C5→C4. The polarizability tensor has accordingly slightly larger Eigenvalues for the N1 conformer. The orientation of the main tensor axes is similar and the contribution in the C5–C4 direction is about 40% smaller than in the N1–C8 direction. On the contrary, in the case of N7-guanine, the HOMO (of π character) lies slightly closer to the vacant 5d-AO of the isolated Pt^{2+} cation, which enables a stronger dative interaction. In this way strength of both the Pt–N bonds is similar. It also correlates with the lower CT from cytosine to Pt atom in structures with G(N1) base (cf. below).

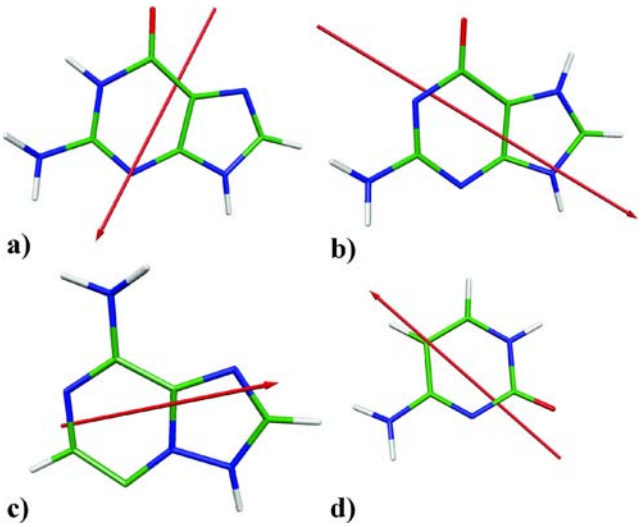

Fig. 2 Optimized conformers of DNA bases and their dipole moments: (**a**) N7-guanine, (**b**) N1-guanine, (**c**) adenine, (**d**) cytosine

The influence of the *trans* effect can be found in the case of *trans*platin coordination with N1(G), where a higher affinity of cytosine leads to the weakest Pt–N(G) bond. This effect is usually not as pronounced since some other energy terms (like H–bond or sterical repulsion) compensate it.

The strength of the Pt–N7(G) bond also reflects the donation ability of the DNA bases examined. As to stabilization energies, both ΔE^{Stab} and ΔE^{Stex} values increase in the order adenine<cytosine<guanine, which is in accord with the most abundant occurrence of 1,2-GpG cross-links (structure **3a**) in real (in vivo or in vitro) assays. The stabilization is, however, a too complex criterion for a more detailed insight and better correlation with the changes of Pt–N7(G) bonding is given by BE characteristics. It can be noticed that the weakest Pt–N7 coordination occurs in diguanine complexes due to the highest mutual bonding competition. In the cytosine–guanine complexes, the Pt–N7 bonds are by about 5 kcal mol^{-1} (on average) stronger. The weakest competition comes from adenine enabling strong Pt–N7(G) bonds (≈113 kcal mol^{-1}). The BE of Pt–N7(A) bonds is only about 91 kcal mol^{-1} and this fact is in good agreement with the very small dipole moment of isolated adenine.

The thermodynamics (Gibbs heat of reaction) of aqua-ligand replacement by the second DNA bases is evaluated in Table 5. We concentrated on the second step since the first one was already treated in previous work [58] where the reaction energy (ΔE) was estimated to be 51 for adenine and 72 kcal mol^{-1} for guanine (at a slightly worse level—MP2/6-31+G(d)) with diaqua-*cis*platin as a reactant. Also, the second reaction step is energetically comparable with previously calculated head-to-head systems: Pt-adenine+guanine (59 kcal mol^{-1}), Pt-guanine+adenine (39 kcal mol^{-1}), and Pt-guanine+guanine (52 kcal mol^{-1}). In our study, the Gibbs energies are systematically about 3–4 kcal mol^{-1} lower than these reaction energies.

From Table 5 it can be noticed that the smallest reaction Gibbs energies are for water replacement by adenine—about 41 kcal mol^{-1}. Smaller reaction energies were also obtained for cytosine replacement in both N7 and N1 *cis*platin+guanine adducts (below 54 and 50 kcal mol^{-1}, respectively). The largest amount of energy is for guanine

Table 5 Reaction energies ΔE and Gibbs energies ΔG for the reaction (in kcal mol^{-1}): Pt–a$_2$wB+B′→Pt–a$_2$BB′+water

Reactants		Products	ΔE	ΔG
cis-Pt–a$_2$wA(N7)	+G →	*cis*-Pt–a$_2$G(N7)A(N7) (HH)	−63.1	**−60.7**
	+G →	*cis*-Pt–a$_2$G(N7)A(N7) (HT)	−62.2	**−59.7**
trans-Pt–a$_2$wA(N7)	+G →	*trans*-Pt–a$_2$G(N7)A(N7) (HT)	−67.9	**−65.4**
	+G →	*trans*-Pt–a$_2$G(N7)A(N7) (HT)	−67.1	**−64.4**
cis-Pt–a$_2$wC(N3)	+G →	*cis*-Pt–a$_2$G(N7)C(N3) (HH)	−66.4	**−65.4**
	+G →	*cis*-Pt–a$_2$G(N7)C(N3) (HT)	−63.0	**−61.9**
trans-Pt–a$_2$wC(N3)	+G →	*trans*-Pt–a$_2$G(N7)C(N3) (HH)	−64.9	**−62.3**
	+G →	*trans*-Pt–a$_2$G(N7)C(N3) (HT)	−68.5	**−65.4**
cis-Pt–a$_2$wG(N7)	+G →	*cis*-Pt–a$_2$G(N7)G(N7) (HH)	−60.1	**−58.3**
	+G →	*cis*-Pt–a$_2$G(N7)G(N7) (HT)	−63.1	**−61.4**
trans-Pt–a$_2$wG(N7)	+G →	*trans*-Pt–a$_2$G(N7)G(N7) (HH)	−56.7	**−55.8**
	+G →	*trans*-Pt–a$_2$G(N7)G(N7) (HT)	−64.0	**−61.6**
cis-Pt–a$_2$wG(N7)	+A →	*cis*-Pt–a$_2$G(N7)A(N7) (HH)	−44.5	**−41.9**
	+A →	*cis*-Pt–a$_2$G(N7)A(N7) (HT)	−43.6	**−40.9**
trans-Pt–a$_2$wG(N7)	+A →	*trans*-Pt–a$_2$G(N7)A(N7) (HT)	−44.8	**−41.7**
	+A →	*trans*-Pt–a$_2$G(N7)A(N7) (HT)	−44.1	**−40.8**
cis-Pt–a$_2$wG(N7)	+C →	*cis*-Pt–a$_2$G(N7)C(N3) (HH)	−56.6	**−54.1**
	+C →	*cis*-Pt–a$_2$G(N7)C(N3) (HT)	−53.2	**−50.6**
trans-Pt–a$_2$wG(N7)	+C →	*trans*-Pt–a$_2$G(N7)C(N3) (HH)	−55.7	**−52.6**
	+C →	*trans*-Pt–a$_2$G(N7)C(N3) (HT)	−59.3	**−55.7**
cis-Pt–a$_2$wC(N3)	+G →	*cis*-Pt–a$_2$G(N1)C(N3) (HH)	−54.4	**−53.2**
	+G →	*cis*-Pt–a$_2$G(N1)C(N3) (HT)	−63.7	**−62.9**
trans-Pt–a$_2$wC(N3)	+G →	*trans*-Pt–a$_2$G(N1)C(N3) (HH)	−59.1	**−56.1**
	+G →	*trans*-Pt–a$_2$G(N1)C(N3) (HT)	−61.9	**−58.7**
cis-Pt–a$_2$wG(N1)	+C →	*cis*-Pt–a$_2$G(N1)C(N3) (HH)	−44.0	**−42.7**
	+C →	*cis*-Pt–a$_2$G(N1)C(N3) (HT)	−53.4	**−52.3**
trans-Pt–a$_2$wG(N1)	+C →	*trans*-Pt–a$_2$G(N1)C(N3) (HH)	−52.4	**−50.1**
	+C →	*trans*-Pt–a$_2$G(N1)C(N3) (HT)	−55.2	**−52.7**

In all cases the N7-conformer of guanine was considered.

replacement, which is in good accord with BE values. Practically all reactions where water was replaced by guanine have reaction energies above 58 kcal mol^{-1}. The most exothermic reactions are in the case where *cis*-Pt–a$_2$G(N7)C(N3) adducts are formed. Here energies of about 64 kcal mol^{-1} are released in the reaction course.

Charge distribution and electrostatic potentials

An investigation of charge distributions and MO analysis in systems give a deeper insight into system interactions. Therefore, NPA partial charges of key elements are shown in Table 2 and dipole moments, main axes of the polarizability tensor, and MO characteristics of isolated bases in Table 6. The orientation of the dipole moments can be seen in Fig. 3. As to the central Pt atom, the decrease in its charge reflects the extent of electron density donation from ammonia molecules and nucleobases. Simultaneously, changes in nitrogen charge of the ligands give an insight into the ratio of donation of individual Pt–N bonds in the complex. However, these criteria are not straightforward since back-donation occurs in the case of DNA bases, as discussed below.

The most positive Pt charge (about 0.69 e) was found in Pt_a$_2$GG systems. This points to a relatively smaller donation from the guanine bases in comparison with the other nucleobases explored, which can be ordered as follows: Pt_a$_2$GA (averaged Pt charge 0.673 e)≈Pt_a$_2$G(N^7)C(N^3) (0.673 e)>Pt_a$_2$G(N^1)C(N^3) with significantly lowest charges (0.656 e). The strength of Pt–N bonds can

Table 6 Electron properties of the used DNA bases: dipole moment μ (in D), main axes of polarizability tensor α (in Å^3), and eigenvalues (in a.u.); N7G means the regular guanine form, N1G labels the N1-tautomer (with protonated N7 site), C-cytosine, and A-adenine

	Pt(II)	N7G	N1G	C	A
μ		6.8	9.5	5.9	4.8
α (xx)		19.8	21.4	15.1	18.0
α (yy)		16.3	16.9	11.6	15.7
α (zz)		7.7	7.8	6.1	7.4
π*(base)		0.09	0.10	0.08	0.09
π*(LUMO)	−0.66	−0.03	0.03	0.05	0.06
π(HOMO)	−1.12	−0.30	−0.30	−0.32	−0.28
π(HOMO-1)		−0.41	−0.34	−0.39	−0.34
σ (HOMO-2)		−0.43	−0.38	−0.41	−0.41

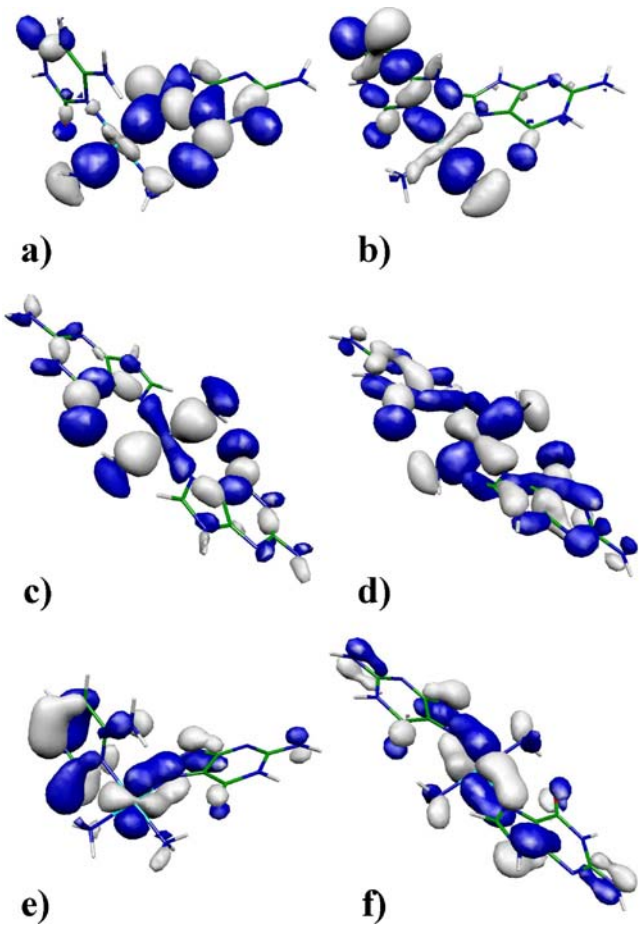

Fig. 3 Molecular orbitals with donation (**a**–**d**) and back-donation (**e**, **f**) characters for *cis*-Pt–a_2G(N7)C(N3) (HH) (**a**, **b**, **e**) and *trans*-Pt–a_2GG (HT) (**c**, **d**, **f**) conformations

be explained as the sum of a dative interaction and electrostatic forces, which are large in the guanine case (especially for the N1-conformer, notice its dipole moment in Table 6). From Table 2, polarization effects can be deduced from the changes in partial charges on the selected atoms. The largest decrease in partial charge occurs at the adenine N1 site, where the averaged difference against the isolated base is 0.08 e. The calculated tensor axes of base polarizability decrease as follows: N1-guanine>N7-guanine>adenine>cytosine as can be seen from Table 6 and Fig. 2, where dipole moments and main axes of the polarizability tensors are shown together with important MO Eigenvalues of isolated DNA bases.

The higher donation activity of the N7 atom of guanine in comparison with the N1 site of the N1-tautomer is related to the Eigenvalues of the highest occupied sigma (HOS) MO, where there is a strong localization of electron density on the interacting N-atom. This is in all cases examined the HOMO-2 orbital. The HOSMO of isolated N7-guanine has its Eigenvalue (of ε=−0.430 a.u.) closest to the vacant 5d-AO of Pt^{2+} (ε=−0.660 a.u.), clearly pointing to a higher donation than in the case of N1-guanine (with corresponding ε=−0.375 a.u.).

The strength of Pt–N coordination also correlates closely with the total charge transfer (CT) from a ligand to Pt atom. These values are included for DNA bases in the last column of Table 2. Here one can notice that CT from cytosine to Pt is larger (on average 0.334 e) for Pt–a_2G(N7)C(N3) complexes, while a smaller CT value of 0.325 e can be found for Pt–a_2G(N1)C(N3) complexes. Comparing CT from adenine and guanine in mixed Pt–GA systems, the CT from adenine is larger than CT from guanine only in the case of the *cis*-Pt–a_2GA (HH) complex. This is connected with the additional interbase donation from O6 of guanine to the NH_2 group of adenine, increasing its total charge. Nevertheless the larger preference for adenine donation over guanine one can be clearly seen from the E(2) perturbation energy approach in the NBO framework. While the interaction energy for donation from N7(A)→Pt is about 5.5, the corresponding value for N7(G)→Pt is only 3.8 kcal mol^{-1}. The energies for back donation from Pt→N7 are similar (70.1 (A) vs. 69.4 (G) kcal mol^{-1}).

When *cis* and *trans* conformers are compared, the donation (according to the decrease in Pt charge) is usually more pronounced in the *trans* structures. This explains the usually higher ΔE^{BE} energies of bases for *trans*platin complexes (the exceptions are caused by additional stabilization due to a higher number of H–bonds or sterical repulsion of the bases). Such a situation differs from "small" ligand (like NH_3 or H_2O) complexes where the *trans*-effect leads to a decrease in bonding energies. The reason for the difference is the fact that back-donation from the Pt AO with π-character to an antibonding π*-MO of bases is allowed (cf. Fig. 3e,f). Such π*-MOs are not available in ammonia or water.

Another insight into these effects can be obtained from charges of the bound nitrogen atoms, which vary according to the ligand type. While the negative charge of the N atom of the ammine ligand increases by about 0.06 e (less negative in coordination) in comparison with isolated ammonia, the N7/N3/N1 charge of the nucleobases is decreased upon coordination to Pt. This corresponds to the different characters of coordination of ammine-ligands and bases where back-donation makes the Pt–N(base) stronger. The decrease in partial charge due to polarization and back-donation is about 0.04 e on the N7 atom of guanine, 0.03 e on N3 of cytosine, and 0.01 e on N7 of adenine.

In *trans*-Pt–a_2GG (HH) structure (Fig. 1 structure **3c**), one of the N(ammine) charges is significantly lower (by about 0.1 e in comparison with isolated ammonia), since both bases are H–bonded to that ligand. This enables a higher donation of the ammine to the Pt atom with an exceptionally short Pt–N(ammine) distance −2.055 Å, even shorter than the Pt–N(base) one in this complex.

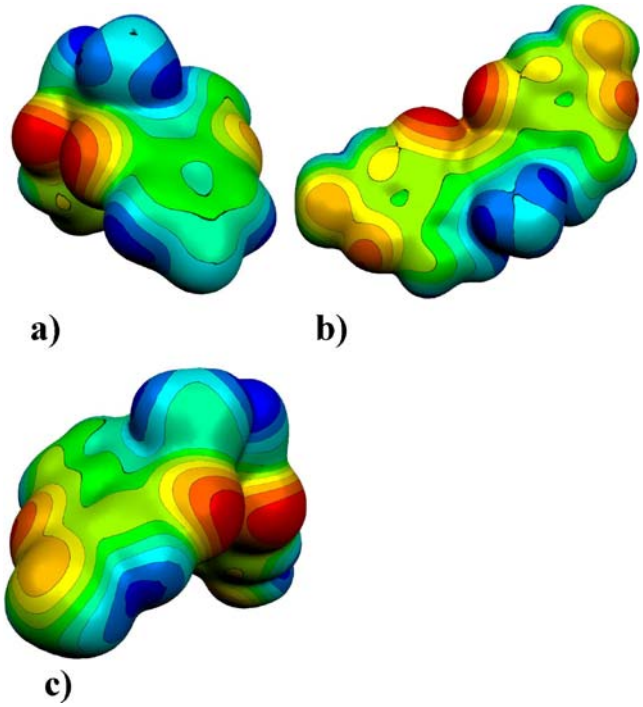

Fig. 4 Maps of electrostatic potentials on isodensity surface (ρ=0.001 electron/Bohr^3) for **a** *cis*-Pt–a$_2$G(N1)C(N3) (HH), **b** *trans*-Pt–a$_2$GG (HH), **c** *cis*-Pt–a$_2$GG (HH)

The remainder of the selected partial charges listed in Table 2 should demonstrate the extent of polarization of the DNA bases. In comparison with isolated bases, the shift of electron density towards the metal cation is clearly evident.

A manifestation of donation and back donation can be seen in the analysis of MOs of two Pt-complexes: *cis*-Pt–a$_2$G(N7)C(N3) (HH) and *trans*-Pt–a$_2$GG (HT). MOs with donation N→Pt (a–d) and back-donation N←Pt (e) and (f), which are involved in these effects are shown in Fig. 3. One can also notice that MOs with donation lie substantially lower (about −0.85 hartree)[1], while MOs with back-donation are about −0.70 hartree. For all the complexes explored electrostatic potentials were also determined. This potential was mapped onto the isodensity surface with ρ=0.001 e/Å^3. The plots obtained give illustrative insight into electrostatic repulsion of various (usually negatively charged) sites of bases involved in platinum complexes. In Fig. 4 three selected cases with the highest repulsions were chosen. The *cis*-Pt–a$_2$G(N1)C(N3) (HH) complex (Fig. 4a), which according to Table 4 exhibits a relatively modest electrostatic repulsion, has both oxygen atoms in close proximity. However, their actual repulsion is partially compensated by an interbase H–bond, as can be seen in Fig. 1 (structure **4a**). The *trans*-Pt–a$_2$GG (HH) complex belongs to systems where only weak H–bonds are present. Here the O6...O6 repulsion causes the largest steric repulsion between the two bases (Fig. 4b). A similar situation also occurs in the *cis*platin analog (*cis*-Pt–a$_2$GG (HH) Fig. 4c), where the second largest repulsion was achieved. The large electrostatic repulsion is usually (at least partially) removed in real assays since additional restrictions due to the sugar-phosphate backbone are present.

Canonical vibrational modes in the harmonic approximation were analyzed in order to obtain an estimate of the H–bond strength. From Table 7, it can be observed that the symmetrical stretching mode of isolated ammonia (estimated ca 3438 cm^{-1} at the DFT/6-31+G(d) level) was shifted below 3200 cm^{-1} in four systems: *cis*-Pt–a$_2$GA (HT) (3145 cm^{-1}), *cis*-Pt–a$_2$G(N7)C(N3) (HT) (3155 cm^{-1}), *trans*-Pt–a$_2$G(N7)C(N3) (HH) (3173), and *cis*-Pt–a$_2$GG (HT) (with 3179 and 3184 cm^{-1}). Therefore, strong additional stabilization must be expected in these complexes. Structures with (ammine)N–H...N6(adenine) and (ammine) N–H...O2(cytosine) interactions were not shifted so profoundly. An interesting situation occurs when comparing C=O6(guanine) and C=O2(cytosine) bond-stretching modes. While in isolated guanine the vibrational frequency is 1799 cm^{-1}, the N1-tautomer has the corresponding value $\tilde{\nu} = 1709\,cm^{-1}$ under the deprotonation of N1 site. This is due to the changes in π-conjugation of the six-membered ring (a partial double bonding character of the N1–C6 bond) shifting the character of the C=O double bond towards a single bond. Platination of the N1 site withdraws some electron density from N1, shifting the frequency back to the regular guanine form. The same effect can also be noticed in complexes containing cytosine, where the frequency shift from the H...O2 H–bond (towards lower values) competes with the shift from π-conjugation, and therefore both positive and negative deviations of the C=O frequency of isolated cytosine (ca 1777 cm^{-1}) can be noticed. Similarly, the C=O frequency of protonated cytosine is 1876 cm^{-1}. The only decreased frequency of the C=O bond occurs in *cis*-Pt–a$_2$G(N1)C(N3) (HT) structure, where two (strong) interbase H–bonds are present (see also the lowest C=O frequency of N1-guanine and extremal values of both Pt–N BEs in this case).

Conclusions

In this work, the DFT optimization at the B3LYP/6-31G(d) level was performed for various platinum cross-links with two DNA bases. These structures occur in many *cis*/*trans*-platinated double-helixes or single-stranded adducts. Nevertheless, no steric hindrance from the sugar-phosphate backbone or other surroundings is considered in the present models. These restrictions could modify the bonding

[1] 1 hartree = 27.211 eV = 627.51 kcal mol-1 = 2625.5 kJ mol-1

Table 7 Vibration frequencies of N–H, C–N6, and C=O bonds involved in H–bonding interactions (in cm^{-1})

Complex	ν_1		ν_2		ν_3		ν_4	
cis-Pt–a_2G(N7)A(N7) (HH)	3434	N6H...O6	3234	aH...N6	1626	C–N6	1763	C=O6
cis-Pt–a_2G(N7)A(N7) (HT)	3145	aH...O6	3238	aH...N6	1626	C–N6	1757	C=O6
trans-Pt–a_2G(N7)A(N7) (HT)	3232	aH...O6	3278	aH...N6	1628	C–N6	1752	C=O6
trans-Pt–a_2G(N7)A(N7) (HT)	3217	aH...O6	3285	aH...N6	1628	C–N6	1756	C=O6
cis-Pt–a_2G(N7)C(N3) (HH)	3198	aH...O6	3367	aH...O2	1754	C=O6	1776	C=O2
cis-Pt–a_2G(N7)C(N3) (HT)	3155	aH...O6	3388	aH...O2	1758	C=O6	1786	C=O2
trans-Pt–a_2G(N7)C(N3) (HH)	3173	aH...O6	3356	aH...O2	1759	C=O6	1781	C=O2
trans-Pt–a_2G(N7)C(N3) (HT)	3381	aH...O6	3368	aH...O2	1741	C=O6	1780	C=O2
cis-Pt–a_2G(N7)G(N7) (HH)	3212	aH...O6	3218	aH...O6	1757	C=O6	1764	C=O6
cis-Pt–a_2G(N7)G(N7) (HT)	3179	aH...O6	3184	aH...O6	1757	C=O6	1760	C=O6
trans-Pt–a_2G(N7)G(N7) (HH)	3284	aH...O6	3320	aH...O6	1764	C=O6	1782	C=O6
trans-Pt–a_2G(N7)G(N7) (HT)	3229	aH...O6	3233	aH...O6	1757	C=O6	1759	C=O6
cis-Pt–a_2G(N1)C(N3) (HH)	3352	aH...O6	3486	N4H...N2	1759	C=O6	1777	C=O2
cis-Pt–a_2G(N1)C(N3) (HT)	3323	N4H...O6	3483	N2H...O2	1724	C=O6	1758	C=O2
trans-Pt–a_2G(N1)C(N3) (HH)	3294	aH...O6	3409	aH...O2	1742	C=O6	1786	C=O2
trans-Pt–a_2G(N1)C(N3) (HT)	3351	aH...O6	3392	aH...O2	1733	C=O6	1776	C=O2

Frequencies determined for N–H, C–N6, and C=O bonds in isolated molecules:
$\tilde{\nu}(aH) = 3438\,cm^{-1},\ \tilde{\nu}(N4H) = 3589\,cm^{-1},\ \tilde{\nu}(N6H) = 3596\,cm^{-1},\ \tilde{\nu}(N2H) = 3563\,cm^{-1},$
$\tilde{\nu}(C-N6) = 1675\,cm^{-1},\ \tilde{\nu}(C=O2) = 1777\,cm^{-1},\ and\ \tilde{\nu}(C=O6) = 1799\,cm^{-1}$
aH means vibrational frequency of (ammine)N–H bond, N4H–(cytosine)N4–H bond, N2H–(guanine)N2–H bond, and N6H–(adenine)N6–H bond

picture, but the basic energy characteristics should not be changed substantially.

Using the MP2/6-31++G(2df,2pd) method, it was found that the most stable structures are the diguanine complexes followed by guanine-cytosine Pt-cross-links, roughly 5 kcal mol^{-1} less stable. The adenine-containing complexes are about 15 kcal mol^{-1} below the stability of diguanine structures.

A detailed insight in covalent bond relations is obtained using bonding energies. The coordination competition of different DNA bases can be elucidated from BE values. The strongest Pt–N bonds are formed with guanine molecules—from 105 to 135 kcal mol^{-1} in dependence on orientation and type of the adjacent base. Pt–N3 bonds of cytosine are on average about 100 and Pt–N7 of adenine about 90 kcal mol^{-1}. The order is in agreement with the stabilization energies. From these values, the energies of H–bonds must also be subtracted. Based on previous results and frequency shifts, the strength of H–bonds can be estimated to be up to 15 kcal mol^{-1} due to relatively high polarization effects caused by the metal cation. The energy characteristics are explained using NPA charges, electrostatic potentials, and MO analysis.

Ackowledgments This study was supported by Charles University grant 438/2004/B_CH/MFF, grant NSF-MŠMT ČR 1P05 ME-784, and grant MSM 0021620835. Computational resources from Meta-Centers in Prague, Brno, and Pilsen are acknowledged for access to their excellent supercomputer facilities. Finally, special thanks must be given to the KFCHO department computer cluster administrated by Dr. M. Šimánek.

References

1. Rosenberg B, van Camp L, Trosko JL, Mansour VH (1969) Nature 222:385–391
2. Beljanski V, Villanueva JM, Doetsch PW, Natile G, Marzilli LG (2005) J Am Chem Soc 127:15833–15842
3. Najajreh Y, Kasparkova J, Marini V, Gibson D, Brabec V (2005) J Biol Inorg Chem 10:722–731
4. Marini V, Christofis P, Novakova O, Kasparkova J, Farrell N, Brabec V (2005) Nucleic Acids Res 33:5819–5828
5. Bhattacharyya D, Marzilli PA, Marzilli LG (2005) Inorg Chem 44:7644–7651
6. Brabec V, Kasparkova J (2005) Drug Resistance Updates 8:131–146
7. Malina J, Voitiskova M, Brabec V, Diakos CI, Hambley TW (2005) Biochem Biophys Res Commun 332:1034–1041
8. Bivian-Castro EY, Roitzsch M, Gupta D, Lippert B (2005) Inorganica Chimica Acta 358:2395–2402
9. Barnes KR, Lippard SJ (2004) Metal complexes in tumor diagnosis and as anticancer agents. In: Metal ions in biological systems, vol 42. pp 143–177
10. Carlone M, Marzilli LG, Natile G (2005) Europ J Inorg Chem 1264–1273
11. Kaim W, Schwederski B (1994) Bioinorganic chemistry: inorganic elements in the chemistry of life. Wiley, Chichester, England
12. Takahara PM, Rosenzweig AC, Frederick CA, Lippard SJ (1995) Nature 377:649–655
13. Takahara PM, Frederick CA, Lippard SJ (1996) J Am Chem Soc 118:12309–12321
14. Yang D, van Boom SSGE, Reedijk J, van Boom JH, Wang AH-J (1995) Biochemistry 34:12912–12921
15. Gelasco A, Lippard SJ (1998) Biochemistry 37:9230–9238
16. Dunham SU, Dunham SU, Turner CJ, Lippard SJ (1998) J Am Chem Soc 120:5395–5403
17. Wing RM, Pjura P, Drew HR, Dickerson RE (1984) EMBO J 3:1201–1212

18. Lilley DMJ (1996) J Biol Inorg Chem 1:189–191
19. Coste F, Malinge JM, Serre L, Shepard W, Roth M, Leng M, Zelwer C (1999) Nucleic Acids Res 27:1837–1845
20. Spingler B, Whittington DA, Lippard SJ (2001) Inorg Chem 40:5596–5602
21. Silverman AP, Bu W, Cohen SM, Lippard SJ (2002) J Biol Chem 277:49743–49754
22. Parkinson GN, Arvanitis GM, Lessinger L, Ginell SL, Jones R, Gaffney B, Berman HM (1995) Biochemistry 34:15487–15495
23. Ohndorf U-M, Rould MA, He Q, Pabo CO, Lippard SJ (1999) Nature 399:708–712
24. Jamieson ER, Lippard SJ (1999) Chem Rev 99:2467–2498
25. Kašparková J, Mackay FS, Brabec V, Sadler PJ (2003) J Biol Inorg Chem 8:741–745
26. Choi S, Delaney S, Orbai L, Padgett EJ, Hakemian AS (2001) Inorg Chem 40:5481–5482
27. Junicke H, Bruhn C, Kluge R, Serianni AS, Steinborn D (1999) J Am Chem Soc 121:6232–6241
28. Song R, Kim KM, Lee SS, Sohn YS (2000) Inorg Chem 39:3567–3571
29. Watanabe M, Kai M, Asanuma S, Yoshikane M, Horiuchi A, Ogasawara A, Watanabe T, Mikami T, Matsumoto T (2001) Inorg Chem 40:1496–1500
30. Kelland LR, Jones MM, Abel G, Harrap KR (1992) Cancer Chemother Pharmacol 30:43–50
31. Wong E, Giandomenico CM (1999) Chem Rev 99:2451–2466
32. Reedijk J (1996) Chem Commun 7:801–806
33. Reedijk J (1999) Chem Rev 99:2499–2510
34. Brabec V, Neplechova K, Kasparkova J, Farell N (2000) J Biol Inorg Chem 5:364–368
35. Sigel H, Song B, Oswald G, Lippert B (1998) Chem Eur J 4:1053–1060
36. Williams KM, Scarcia T, Natile G, Marzilli LG (2001) Inorg Chem 40:445–454
37. Paquet F, Perez C, Leng M, Lancelot G, Malinge JM (1996) J Biomol Struct Dyn 14:67–77
38. Huang HF, Zhu LM, Reid BR, Drobny GP, Hopkins PB (1995) Science 270:1842–1845
39. Payet D, Gaucheron F, Sip M, Leng M (1993) Nucleic Acids Res 21:5846–5859
40. Bancroft DP, Lepre CA, Lippard SJ (1990) J Am Chem Soc 112:6860–6867
41. Monjardet-Bas V, Chottard J-C, Kozelka J (2002) Chem Eur J 1144–1150
42. Perez C, Leng M, Malinge JM (1997) Nucleic Acids Res 25:896–903
43. Reedijk J (1992) Inorg Chim Acta 198:873–876
44. Brabec V, Leng M (1993) Proc Natl Acad Sci USA 90:5345–5346
45. Paquet F, Boudvillain M, Lancelot G, Leng M (1999) Nucleic Acids Res 27:4261–4268
46. Comess KM, Costello CE, Lippard SJ (1990) Biochemistry 29:2102–2114
47. Dalbies R, Boudvillain M, Leng M (1995) Nucleic Acids Res 23:949–957
48. Boudvillain M, Dalbies R, Aussourd C, Leng M (1995) Nucleic Acids Res 23:2381–2389
49. Boudvillain M, Guerin M, Dalbies R, Saison-Behmoaras T, Leng M (1997) Biochemistry 36:2925–2936
50. Lippert B (1999) *Cis*platin: chemistry and biochemistry of a leading anticancer drug. Wiley-VCH, Weinheim, Germany
51. Martin RB (1983) In: Lippard SJ (ed) Platinum, gold and other metal chemoterapeutic agents, vol 209. ACS Symposium Series, Washington District of Columbia, p 859
52. Arpalahti J, Klika KD, Sillanpaa R, Kivekas R (1998) J Chem Soc, Dalton Trans 1397–1402
53. Carloni P, Sprik M, Andreoni W (2000) J Phys Chem B 104: 823–835
54. Baik M-H, Friesner RA, Lippard SJ (2002) J Am Chem Soc 124:4495–4503
55. Baik MH, Friesner RA, Lippard SJ (2003) J Am Chem Soc 125:14082–14092
56. Eriksson LA, Raber J, Zhu C (2005) J Phys Chem 109:11006–11015
57. Chval Z, Šíp M (2003) Collect Czechoslov Chem Commun 68:1105–1118
58. Burda JV, Leszczynski J (2003) Inorg Chem 42:7162–7172
59. Burda JV, Šponer J, Hrabáková J, Zeizinger M, Leszczynski J (2003) J Phys Chem B 107:5349–5356
60. Zeizinger M, Burda JV, Leszczynski J (2004) Phys Chem Chem Phys 6:3585–3590
61. Deubel DV (2002) J Am Chem Soc 124:5834–5842
62. Burda JV, Zeizinger M, Šponer J, Leszczynski J (2000) J Chem Phys 113:2224–2232
63. Zeizinger M, Burda JV, Šponer J, Kapsa V, Leszczynski J (2001) J Phys Chem A 105:8086–8092
64. Burda JV, Zeizinger M, Leszczynski J (2004) J Chem Phys 120:1253–1262
65. Burda JV, Zeizinger M, Leszczynski J (2005) J Comput Chem 26:907–914
66. Zimmermann T, Zeizinger M, Burda JV (2005) J Inorg Biochem 99:2184–2196
67. Andrae D, Haussermann U, Dolg M, Stoll H, Preuss H (1990) Theor Chim Acta 77:123–141
68. Foster JP, Weinhold F (1980) J Am Chem Soc 102:7211–7218
69. Reed AE, Weinhold F (1983) J Chem Phys 78:4066–4073
70. Reed AE, Weinstock RB, Weinhold F (1985) J Chem Phys 83:735–746
71. Weinhold F (2001) University of Wisconsin, Madison, Wisconsin 53706, Wisconsin